CrystEngComm

ROYAL SOCIETY OF CHEMISTRY

PAPER

View Article Online
View Journal | View Issue

Cite this: *CrystEngComm*, 2025, **27**, 6381

Metal organic framework with high water stability and dense open metal sites for carbon monoxide capture

Yucong Xia,[a] Julia Piper Radtke,[b] Timo Thonhauser,[b] Nathan M. Rabideaux[c] and Jing Li*[ad]

Received 24th July 2025,
Accepted 3rd September 2025

DOI: 10.1039/d5ce00741k

rsc.li/crystengcomm

We report the synthesis, characterization and carbon monoxide (CO) adsorption properties of a series of isoreticular and water-stable metal–organic frameworks M_2Cl_2(bbta) (M = Co, Mn, Cu), composed of a one-dimensional (1D) metal-chloride chain building unit and a triazolate linker. Among them, Co_2Cl_2(bbta) exhibits the most promising performance for CO capture. Featuring a high density of open cobalt sites (3.8 nm^{-3}), Co_2Cl_2(bbta) takes up 3.06 mmol g^{-1} of CO at 298 K, with a high isosteric heat of adsorption (Q_{st}) of 35 kJ mol^{-1}, indicating strong interaction at the Co(II) centers. This interaction as a function of loading is further analyzed with the help of *ab initio* calculations. Remarkably, the framework maintains structural integrity and adsorption capacity after prolonged water exposure and multiple adsorption–desorption cycles. These results highlight Co_2Cl_2(bbta) as an example of a hydrolytically stable, OMS-rich MOF suitable for reversible CO capture. Its durability, regenerability, and strong affinity for CO make it a promising candidate for real-world gas separation and storage applications.

Introduction

Carbon monoxide (CO) is a colorless, odorless, and tasteless gas that poses a significant threat to human health and safety due to its high toxicity and prevalence in both industrial and residential environments. Produced primarily from incomplete combustion of carbon-containing fuels, CO is a major component of exhaust gases from automobiles, power plants, and furnaces.[1] CO binds to hemoglobin with an affinity over 200 times greater than that of oxygen (O_2). As a result, exposure to CO can significantly impair the transport of oxygen in the human bloodstream, leading to symptoms ranging from headaches and dizziness to unconsciousness, and even death at high concentrations.[2] Due to its high toxicity even at low concentrations, regulatory agencies such as the U.S. Environmental Protection Agency (EPA) have set stringent limits for ambient CO levels—currently 9 ppm over 8 hours and 35 ppm over 1 hour.[3]

In industrial settings, CO is an important reactant and product in processes such as syngas production, Fischer–Tropsch synthesis, and hydroformylation.[4] Effective CO adsorption and removal technologies are therefore essential for both safety and process efficiency. Traditional adsorbents such as activated carbons and zeolites suffer from limitations in selectivity, capacity, and chemical tunability. In recent years, metal–organic frameworks (MOFs) have emerged as a promising class of materials for CO adsorption, capture and separation due to their high surface areas, tunable pore structures, and chemical versatility.[5,6]

MOFs constructed with coordinatively unsaturated metal centers—commonly referred to as open metal sites (OMS)—are particularly well-suited for CO adsorption. These sites provide strong binding interactions through σ-donation and π-backbonding mechanisms, enabling high affinity toward CO molecules.[7–11] A higher density of OMS typically correlates with greater adsorption capacity and more efficient separation performance.

Despite these advantages, many MOFs with high OMS densities are susceptible to degradation under humid conditions. Water molecules can compete with CO for binding at metal centers and, in many cases, compromise the structural integrity of the framework.[12] This vulnerability greatly limits the practical application of OMS-rich MOFs in real-world environments, where exposure to moisture is inevitable.

In this study, we present the synthesis, characterization and CO adsorption properties of Co_2Cl_2(bbta) (H_2bbta = 1*H*,5*H*-benzo(1,2-*d*:4,5-*d*′)bistriazole). We systematically

[a] *Department of Chemistry and Chemical Biology, Rutgers University-New Brunswick, 123 Bevier Road, Piscataway, New Jersey 08854, USA. E-mail: jingli@rutgers.edu*
[b] *Department of Physics and Center for Functional Materials, Wake Forest University, 1834 Wake Forest Rd, Winston-Salem, North Carolina 27109, USA*
[c] *Department of Chemistry, Rutgers University-Newark, 73 Warren Street, Newark, New Jersey 07102, USA*
[d] *Department of Information Display, Kyung Hee University, 26 Kyungheedae-ro, Dongdaemun-gu, Seoul 02447, Republic of Korea*

evaluate the material's structural stability under aqueous conditions and assess its CO binding strength using a combination of spectroscopic and gas adsorption techniques. This work aims to contribute to the development of next-generation MOFs that bridge the gap between performance and durability for gas adsorption applications.

Results and discussion

Microcrystalline powders of Co_2Cl_2(bbta) were synthesized according to a previously reported procedure with some modification.[13] A solution of the ligand H_2bbta (20 mg, 0.125 mmol, 1 eq.) and hydrochloric acid (0.1 mL) in *N*,*N*′-dimethylformamide (4 mL) was added to a solution of $CoCl_2 \cdot 6H_2O$ (30 mg, 0.32 mmol, 2.5 eq.) in methanol (4 mL) in a 20 mL autoclave with a Teflon-lined cap and heated for 3 d in a 65 °C oven. After allowing the reaction to cool, it was filtered and the precipitate was resuspended in fresh methanol (20 mL) in a glass vial. The vial was heated in an oven at 60 °C for 3 days, and every 12 h the solvent was filtered off and replaced. After 3 days, the pink precipitate was filtered to dryness and evacuated at room temperature for 24 h, before being heated to 100 °C under vacuum for another 12 h. Scanning electron microscopy (SEM) analysis of the resulting product revealed the uniform production of hexagonal rods with a high aspect ratio (Fig. S1). In addition to the cobalt-based framework, isostructural M_2Cl_2(bbta) compounds (M = Mn and Cu) were also successfully synthesized.

The M_2Cl_2(bbta) MOF series were characterized by powder X-ray diffraction (PXRD) method, which confirmed that the materials are isostructural with previously reported analogues (Fig. 2a). Among these, Co_2Cl_2(bbta) was selected for further investigation due to its significantly higher CO uptake compared to its Mn- and Cu-based counterparts. Structural analysis of Co_2Cl_2(bbta) revealed that each cobalt ion adopts a distorted octahedral coordination geometry, ligated by three nitrogen atoms from three distinct bbta ligands, two chloride anions, and one terminal solvent molecule. Each bbta ligand bridges six cobalt centers through its triazolate rings. The framework features helical chains of cobalt ions interconnected *via* μ_3-triazolate linkages and bridging chloride anions. These chains are further connected through the phenylene backbones of the bbta ligands to generate a three-dimensional (3D) structure containing 1D open channels (with large hexagon-shaped cross sections) parallel to the helical chains (Fig. 1). The solvent molecules that bind these cobalt centers can be removed by heating under vacuum, generating five-coordinate cobalt sites with a density of 3.8 nm^{-3}. These open metal sites are accessible to guest molecules and play a critical role in CO adsorption, providing strong, specific interactions that contribute to the material's high CO uptake capacity.

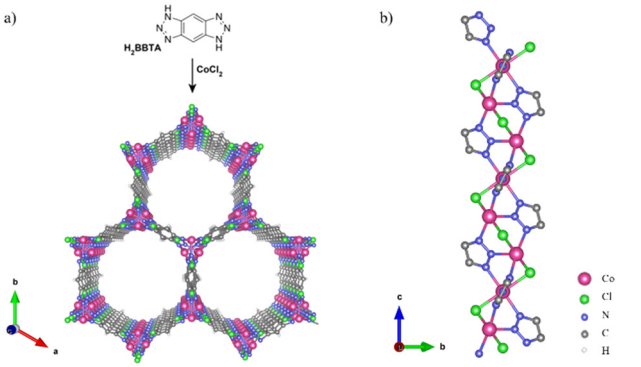

Fig. 1 (a) Crystal structure of Co_2Cl_2(bbta) viewed along the *c*-axis. (b) Structure of a helical cobalt-chloride–triazolate chain running along the *c*-axis (Co, pink; Cl, green; N, blue; C, grey; H, white).

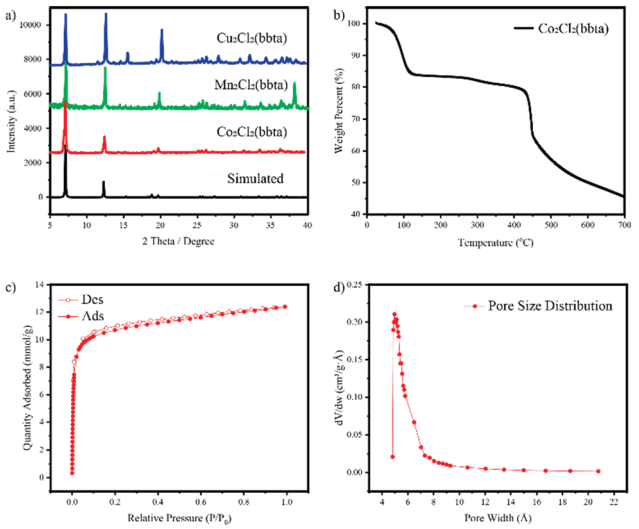

Fig. 2 (a) PXRD patterns of M_2Cl_2(bbta). (b) The TGA plots of Co_2Cl_2(bbta). (c) CO_2 adsorption–desorption isotherms of Co_2Cl_2(bbta) at 195 K, and (d) pore size distribution (H–K function) of Co_2Cl_2(bbta).

The structural characteristics and thermal stability of Co_2Cl_2(bbta) were further examined through thermogravimetric analysis (TGA). Prior to analysis, the as-synthesized material underwent a solvent-exchange procedure, in which it was soaked in methanol for three days to replace high-boiling-point solvents (DMF) with more volatile ones (methanol). The TGA profile of the methanol-exchanged sample revealed an initial weight loss of approximately 15.6% occurring below 120 °C, which is attributed to the evaporation of residual methanol and loosely bound guest molecules within the pores (Fig. 2b). Importantly, the framework exhibited thermal stability up to around 300 °C, with no major weight loss observed before this temperature, indicating that the Co_2Cl_2(bbta) framework maintains its integrity well above typical application temperatures. The porosity and accessible pore volume of the activated sample were determined based on CO_2 sorption data collected at 195 K. The resulting isotherm displayed a typical type I behavior, characteristic of microporous materials. From these data, the Brunauer–Emmett–Teller (BET) surface area was calculated to be approximately 800 $m^2\ g^{-1}$ (Fig. 2c). Further analysis of the

pore structure using the Horvath–Kawazoe (H–K) model yielded an average pore diameter of 5.0 Å, consistent with a uniform microporous network (Fig. 2d).

To evaluate the water stability of Co_2Cl_2(bbta), a long-term immersion test was conducted in which the activated sample was submerged in water and stored under ambient conditions for an extended period of one month. This test aimed to simulate realistic environmental exposure, such as humid atmospheres or long-time water contact, which often compromise the structural integrity of many MOFs. After the immersion period, the recovered sample was thoroughly dried and the structural integrity of the framework was assessed using PXRD analysis. Remarkably, the PXRD patterns obtained after water exposure closely matched that of the pristine material, with no observable peak broadening, shifting, or intensity loss (Fig. S2). This outcome demonstrated that Co_2Cl_2(bbta) retained its crystallographic framework even after prolonged water exposure, confirming its exceptional hydrolytic stability and suggesting its strong resistance to degradation or structural collapse in aqueous environments.

Single-component CO adsorption isotherms were measured at different temperatures to evaluate the adsorption performance of Co_2Cl_2(bbta). Before measurements, solvent exchange was carried out on each sample in MeOH at 60 °C for three days, with the supernatant replaced by fresh MeOH every 12 hours. Activation was subsequently done under dynamic vacuum at 120 °C for 3 hours. Co_2Cl_2(bbta) reached an adsorption capacity of 3.06 mmol g^{-1} (68.3 cm^3 g^{-1} STP) at 298 K, 101.3 kPa while its Mn- and Cu-based analogues can only take up 1.98 mmol g^{-1} and 0.47 mmol g^{-1}, respectively under the same conditions (Fig. 3a). To evaluate the framework's stability and reusability, Co_2Cl_2(bbta) was subjected to multiple CO adsorption–desorption cycles. After each cycle, the sample was soaked in water overnight and reactivated under the same conditions to restore its adsorption capacity. Notably, even after the 8th cycle, the material still retained a substantial CO capacity (Fig. 3b). This resilience under aqueous environment and repeated activation suggests that Co_2Cl_2(bbta) possesses both good performance and robustness, making it a promising candidate for practical applications in reversible CO capture and storage.

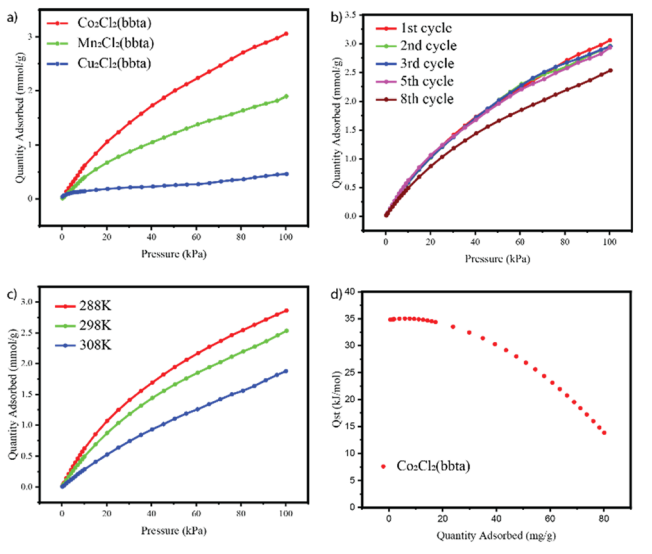

Fig. 3 The single-component CO adsorption isotherms of (a) M_2Cl_2(bbta) (M = Co, Mn, Cu) at 298 K; (b) Co_2Cl_2(bbta) after multiple cycles; (c) Co_2Cl_2(bbta) at 288 K, 298 K and 308 K. (d) The isosteric heats (Q_{st}) of CO adsorption of Co_2Cl_2(bbta) calculated from isotherms collected at 288 K, 298 K and 308 K.

Temperature-dependent adsorption studies further revealed that Co_2Cl_2(bbta) maintained a high capacity across a relevant thermal range (2.86 mmol g^{-1} at 288 K, 101.3 kPa; 1.88 mmol g^{-1} at 308 K, 101.3 kPa) (Fig. 3c). The coverage-dependent isosteric heats of adsorption (Q_{st}) of CO in Co_2Cl_2(bbta) were determined using the Clausius–Clapeyron equation, derived from the series of adsorption isotherms collected at different temperatures. This method enables a precise evaluation of the interaction strength between CO molecules and the adsorption sites within the framework across varying degrees of surface coverage. At near-zero coverage, the calculated isosteric heats (Q_{st}) was approximately 35 kJ mol^{-1}, indicating a strong interaction between CO and the most energetically favorable sites, namely the open cobalt metal centers (Fig. 3d). In contrast to typical physisorption processes—such as those observed for N_2 and CO on inert surfaces—where Q_{st} values are generally below 20 kJ mol^{-1}, the significantly higher values observed at low coverage in Co_2Cl_2(bbta) suggest that the initial uptake of CO is dominated by strong metal–CO interactions. This implies the formation of stronger, possibly coordinate or donor–acceptor bonds between CO molecules and the exposed cobalt sites, rather than simple van der Waals interactions. However, as the CO loading increased and these high-affinity sites became saturated, the Q_{st} gradually decreased to around 15 kJ mol^{-1} at full capacity. This pronounced drop reflects the progressive occupation of weaker adsorption sites and highlights the heterogeneity of the binding environments within the framework. The presence of such specific and strong interactions at low pressures is particularly advantageous for CO capture and underscores the potential of Co_2Cl_2(bbta) as a high-affinity sorbent in gas separation or sensing applications.

To further investigate the guest-host interactions, *ab initio* calculations were performed to provide molecular level mechanistic insights into the adsorption behavior of Co_2Cl_2(bbta) towards CO. The loading of Co_2Cl_2(bbta) with up to three guest molecules of CO was studied, and the binding was compared with that of N_2. The various binding energies can be found in Table S1. The C atom of the CO molecule formed a strong bond with the open Co site of the framework at a distance of 2.34 Å (Fig. 4a). The binding energy of 31 kJ mol^{-1} was in good agreement with the experimental isosteric heat of adsorption (35 kJ mol^{-1}). This arrangement was able

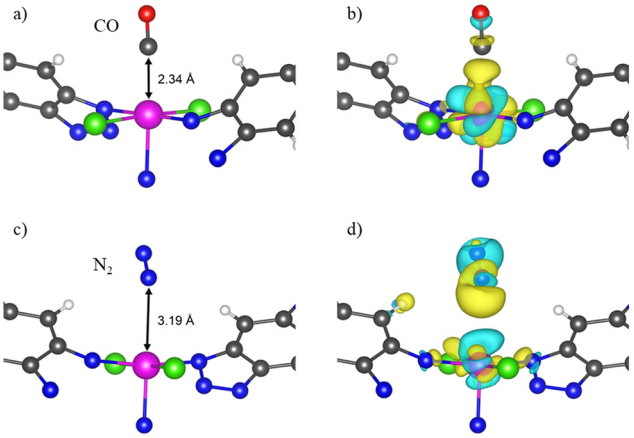

Fig. 4 (a) Binding configuration of CO in Co_2Cl_2(bbta); (b) induced charge density, *i.e.*, the rearrangement of the charge density upon formation of the bond, at an iso-level of 0.003 e Å^{-3}. Yellow lobes show charge accumulation while blue lobes show charge depletion; (c) binding configuration of N_2 in Co_2Cl_2(bbta); (d) induced charge density at an iso-level of 0.0003 e Å^{-3}. Color coding: magenta = Co, green = Cl, blue = N, black = C, red = O, and white = H.

to draw considerable charge into the bond, mostly through rearranging the occupations of the d-like Co orbitals, explaining the strength of the bond. It is interesting to see that the loading of additional CO guest molecules decreased the binding energy per guest molecule somewhat. Nonetheless, cooperative loading of up to 3 CO molecules was energetically very favorable. Additional CO guest molecules binded at nearby open Co sites essentially in the same configuration as a single CO molecule. Table S1 also showed the binding of N_2 to the Co_2Cl_2(bbta) framework, albeit with noticeably weaker binding of only 21 kJ mol^{-1} compared to CO. This N_2 bond was of a different nature, as the molecule cannot interact with the d-like orbitals of Co in the same way (Fig. 4c and d). As a result, noticeable less charge was pulled into the bond and the bond distance increases to 3.19 Å. Interestingly, the binding energy of N_2 was almost independent of the amount of loading.

Conclusions

In this study, we have successfully demonstrated that Co_2Cl_2(bbta) is a water-stable MOF featuring a high density of open cobalt sites (3.8 nm^{-3}), relatively large CO adsorption capacity (3.06 mmol g^{-1} at 298 K), and excellent structural integrity under humid conditions. The framework retains its crystallinity and porosity even after prolonged water exposure and multiple CO adsorption–desorption cycles, affirming its durability in realistic operational environments. Temperature-dependent isotherms and isosteric heats calculations revealed strong interactions between CO and the cobalt centers—which we confirmed and analysed further with the help of *ab initio* simulations—with an isosteric heat of adsorption reaching 35 kJ mol^{-1} at low coverage. These findings position Co_2Cl_2(bbta) as a promising candidate for reversible CO capture. Its unique combination of hydrolytic stability, high CO affinity, and regeneration capacity offers a valuable design blueprint for the development of next-generation MOFs intended for gas separation, purification, and storage. Future work may focus on further tuning the chemical environment around the cobalt sites to enhance selectivity in multicomponent gas mixtures, and to improve the framework's capacity to retain CO within its porous lattice. We also aim at exploring its application as a CO carrier to provide a controllable CO source for industrial organic synthesis.

Author contributions

J. Li and Y. Xia conceived the research idea and formulated the whole project. Y. Xia synthesized the compounds, performed physical characterizations, and collected the CO adsorption data. T. Thonhauser and J. P. Radtke performed DFT calculations. N. M. Rabideaux collected and analyzed SEM images. J. L. supervised the research project. J. Li and Y. Xia coordinated the writing of the manuscript. All authors contributed to the drafting and revising of the manuscript and gave their approval to the final version of the paper.

Conflicts of interest

There are no conflicts to declare.

Data availability

Supplementary information: Full experimental details, physical characterizations, additional gas adsorption measurements and supplemental references. See DOI: **https://doi.org/10.1039/D5CE00741K**

The data supporting this article have been included as part of the SI.

Acknowledgements

We are grateful for the financial support from the U.S. Department of Energy, Office of Science, Office of Basic Energy Sciences under Award No. DE-SC0019902. J. L. is thankful to Kyung Hee University for the Eminent Scholarship.

Notes and references

1 S. Dey and G. C. Dhal, *Mater. Sci. Energy Technol.*, 2019, **2**, 607–623.
2 J. J. Rose, L. Wang, Q. Xu, C. F. McTiernan, S. Shiva, J. Tejero and M. T. Gladwin, *Am. J. Respir. Crit. Care Med.*, 2017, **195**, 596–606.
3 U. S. EPA, *National Ambient Air Quality Standards (NAAQS) for Carbon Monoxide*, **https://www.epa.gov/naaqs/carbon-monoxide-co-air-quality-standards)**.
4 J.-B. Peng, H.-Q. Geng and X.-F. Wu, *Chem*, 2019, **5**, 526–552.

5 J. R. Li, J. Sculley and H. C. Zhou, *Chem. Rev.*, 2012, **112**, 869–932.
6 J. B. DeCoste and G. W. Peterson, *Chem. Rev.*, 2014, **114**, 5695–5727.
7 D. A. Reed, B. K. Keitz, J. Oktawiec, J. A. Mason, T. Runcevski, D. J. Xiao, L. E. Darago, V. Crocella, S. Bordiga and J. R. Long, *Nature*, 2017, **550**, 96–100.
8 A. Evans, R. Luebke and C. Petit, *J. Mater. Chem. A*, 2018, **6**, 10570–10594.
9 X. W. Zhang, C. Wang, Z. W. Mo, X. X. Chen, W. X. Zhang and J. P. Zhang, *Nat. Mater.*, 2024, **23**, 116–123.
10 S. Hu, G. Guo, J. Zhang, M. N. Khan, S. Xu, F. Yang, B. W. Schwandt, Z. Hu and J. Zou, *Mater. Sci. Eng., R*, 2024, **161**, 100874.
11 E. Martinez-Ahumada, M. L. Diaz-Ramirez, M. J. Velasquez-Hernandez, V. Jancik and I. A. Ibarra, *Chem. Sci.*, 2021, **12**, 6772–6799.
12 N. C. Burtch, H. Jasuja and K. S. Walton, *Chem. Rev.*, 2014, **114**, 10575–10612.
13 X. F. Lu, P. Q. Liao, J. W. Wang, J. X. Wu, X. W. Chen, C. T. He, J. P. Zhang, G. R. Li and X. M. Chen, *J. Am. Chem. Soc.*, 2016, **138**, 8336–8339.